

Development of a Transonic Free-to-Roll Test Capability

Francis J. Capone,* D. Bruce Owens,† and Robert M. Hall‡
NASA Langley Research Center, Hampton, Virginia 23681

As part of the NASA/Navy Abrupt Wing Stall Program, a relatively low-cost, rapid-access, free-to-roll test rig was developed on which conventional high-strength wind-tunnel models can be used to evaluate both transonic performance and wing-drop/rock behavior in a single tunnel entry. The overall objective was to demonstrate the utility of the free-to-roll test technique as a tool for identifying areas of significant uncommanded lateral activity during ground testing and for gaining insight into the wing-drop/rock behavior of military aircraft at transonic conditions. A description of the test hardware as well as a description of the experimental procedures is given. The free-to-roll test rig has been used successfully to assess the static and dynamic characteristics of four different configurations—two configurations that exhibited uncommanded lateral motions inflight (preproduction F/A-18E and AV-8B) and two that did not (F/A-18C, F-16C). Excellent agreement between free-to-roll results and flight was obtained for those configurations where flight data were available.

Nomenclature

C_A	= axial-force coefficient
C_l	= rolling-moment coefficient
$C_{l,0}$	= rolling-moment coefficient at $\beta = 0$ deg
C_N	= normal-force coefficient
C_m	= pitching-moment coefficient
C_n	= yawing-moment coefficient
C_Y	= side-force coefficient
M	= Mach number
p	= roll rate
$pb/2V_\infty$	= reduced angular rate
t	= time
V_∞	= freestream velocity
α	= angle of attack, deg
β	= angle of sideslip, deg
δ_a	= aileron angle, deg
δ_{le}	= leading-edge flap angle, deg
δ_{te}	= trailing-edge flap angle, deg
θ	= pitch angle, deg
ϕ	= roll angle, deg

Introduction

FOR more than 50 years, many high-performance military aircraft have experienced abrupt, uncommanded lateral motion during transonic maneuvers.¹ Recently, the preproduction F/A-18E/F experienced wing drop during the development flight-test program. During this extensive flight program, over 100 configurations with 10,000 wind-up turns were evaluated over a period of 1.5 years.² This problem was eventually solved by modifying the wing automatic leading-edge flap schedule and by the addition of a porous fairing at the wing fold location. These fixes have since been incorporated into production versions of the F/A-18E/F aircraft no longer exhibit wing-drop behavior. A Blue Ribbon panel established by the U.S. Department of Defense during this time period concluded that

there was a lack of understanding of the abrupt-wing-stall process on the preproduction F/A-18E/F and that a broad-based research effort should be conducted to systematically study the wing-drop phenomena. They also stated that this research effort should focus on developing figures of merit, design guidelines, and identify and develop appropriate wind-tunnel test techniques and computational codes that would be useful for predicting and solving this problem for future platforms. The Abrupt Wing Stall (AWS) program² was formed to study the unexpected occurrence of highly undesirable lateral-directional motions at high-subsonic and transonic maneuvering conditions, and overall accomplishments of this program are presented in Ref. 3. One of the recommendations from Ref. 1 was to “develop a relatively low-cost, rapid-access wind-tunnel approach that combines the use of conventional models and test apparatuses to evaluate both transonic performance and wing-drop tendencies using the free-to-roll approach in a single tunnel entry.”

The overall objective of the free-to-roll (FTR) test technique is to identify early the potential for uncommanded lateral motions. Together with the static force and moment data, free-to-roll testing can determine the severity of model motions, assess the impact of unsteady and nonlinear aerodynamics (rate and amplitude), and determine dynamic aerodynamic data (roll damping). Figure 1 shows the kinematic interchanges of angle of attack and sideslip during wing-drop. With the model given a degree of freedom in roll, kinematic variations of angles of attack and sideslip occur during the rolling motions.

The free-to-roll test technique has been used by NASA at the Langley Research Center to determine the low-speed, high-angle-of-attack characteristics of high-performance aircraft for over 30 years. One aircraft that exhibited wing-rocking motions at high angles of attack was the F-4 (Ref. 1). The uncommanded lateral motions of the F-4 involved highly nonlinear dynamic effects, which should be considered in any analyses of transonic wing drop/rock. The cause of wing rock on the F-4 was determined to be loss of aerodynamic damping in roll near stall.⁴ Extensive forced oscillation wind-tunnel tests with an F-4 model showed the damping to be slightly unstable at stall and very nonlinear such that, at relatively small amplitudes of roll oscillations (<5 deg) the damping was unstable. In addition, wind-tunnel testing of a free-flying model at low speeds duplicated the wing rock of the full-scale airplane.

During these investigations, researchers observed that the wing-rock motions seen during the free-flight model tests were typically pure rolling motions, as might be expected because aircraft that are inertially “slender” will tend to move about the axis of least resistance—in this case, the roll axis. It was reasoned that the mechanisms of the wing rock might be captured by a simple test method that permitted only rolling motions. In unpublished low-speed tests, the F-4 free-flight model was stung mounted through the rear on a dummy balance, using a bearing to provide a single degree of

Presented as Paper 2003-0749 at the AIAA 41st Aerospace Sciences meeting and Exhibition, Reno, NV, 6 January 2003; received 30 May 2003; revision received 21 October 2003; accepted for publication 4 November 2003. This material is declared a work of the U.S. Government and is not subject to copyright protection in the United States. Copies of this paper may be made for personal or internal use, on condition that the copier pay the \$10.00 per-copy fee to the Copyright Clearance Center, Inc., 222 Rosewood Drive, Danvers, MA 01923; include the code 0021-8669/04 \$10.00 in correspondence with the CCC.

*Senior Research Engineer, Configuration Aerodynamic Branch.

†Research Engineer.

‡Senior Research Engineer, Configuration Aerodynamics Branch. Member AIAA.

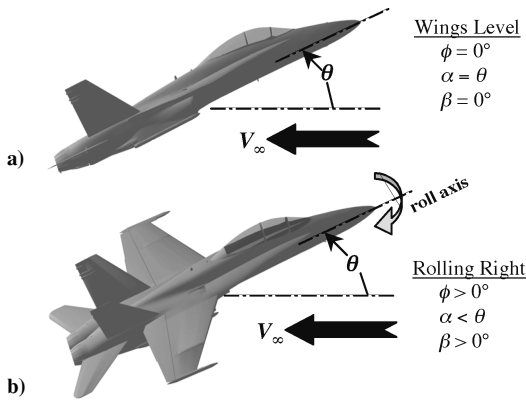


Fig. 1 Kinematic relationships during wing-drop motions.

freedom in roll. The results of these tests showed excellent agreement with the free-flight-test results in terms of angle of attack for onset and also for the amplitude and frequency of motion.

NASA Langley Research Center has also used single-degree-of-freedom free-to-roll wind-tunnel tests to successfully predict rolling motions at low speed and high angles of attack. Low-speed testing of the X-29 forward-swept-wing aircraft⁵ discovered wing rock before flight. This enabled changes to be made to the flight control system to handle the wing rock. Other published free-to-roll studies by NASA Langley include an assessment of the effects of fuselage forebody geometry on stability and control⁶ and wing-rock characteristics of slender delta wings.⁷

The F-5A, F-5E, and T-38 trainer all encountered unexpected wing rock/drop at certain transonic flight conditions in their respective development programs. In a unique experiment in the Ames 11-ft tunnel, Northrop conducted static and semi-free-to-roll tests of an F-5A model to analyze the cause and mechanisms of the wing-rock motions encountered in flight.⁸ Utilizing an $\frac{1}{7}$ -scale buffet model and a special sting with a torsional spring and variable damper, Northrop was able to create, observe, and analyze wing-rock motions exhibited by the full-scale airplane at transonic speeds. Also, different types of uncommanded motions were measured at transonic conditions including limit-cycle, periodic wing rock, and periodic roll activity following a wing-drop event. It was hypothesized⁸ that wing rock could result from either a change from positive to negative aerodynamic damping in roll or from random, aerodynamically forced fluctuating moments caused by unsteady shock movements. With the exception of this semi-free-to-roll test, the use of the FTR test technique has not been used to study uncommanded lateral motions in the transonic speed regime partly because of a lack of appropriate test apparatus.¹

As part of the AWS program, pathfinder tests were conducted in the Langley Transonic Dynamics Tunnel (TDT) on a 9% lightweight composite model of the preproduction F/A-18E using a similar free-to-roll apparatus as used in the F-4 tests. This highly successful pathfinder test proved the utility of the FTR test technique in evaluating the uncommanded lateral motions of the preproduction F/A-18E. However, it was necessary to fabricate a new model for this investigation because the existing free-to-roll apparatus was too large to fit within the existing 8% F/A-18E high-speed force model. In addition, because the free-to-roll apparatus was load limited to 500 lb it was necessary to conduct these tests in the heavy-gas environment in TDT at Reynolds numbers less than 1×10^6 per foot.

Based on these encouraging results, a design effort was initiated to develop a free-to-roll test rig that could handle a variety of conventional wind-tunnel models in a transonic tunnel. A major objective of this design was to utilize the same model and tunnel test apparatus for both static and free-to-roll testing, thereby conducting conventional static and free-to-roll tests in a relatively rapid sequence during a specific tunnel entry. In this regard, the free-to-roll technique offers considerable advantage over other approaches, such as forced oscillation and rotary-balance tests where special models and tunnel entries are required. Of course, after configurations have been

screened the latter tests can still be required to obtain quantitative data on roll damping for simulation and more refined analysis. This paper will discuss the requirements imposed on the new free-to-roll rig as well as describe the hardware arrangement and free-to-roll test technique. Some representative results obtained during the testing of four fighter aircraft models will also be presented.

Description of Free-to-Roll Hardware

Requirements

The major design requirement for the new free-to-roll test rig was to be able to use existing industry high-strength wind tunnel models of varying sizes, weights, and maximum load capabilities. This requirement was imposed so that no separate model would need to be fabricated as had been previously done. Another requirement was the desire to change quickly test modes from conventional static testing to free-to-roll testing. Thus, it was necessary that the force balance be retained such that no additional setup time would be required when changing test modes. Even though there were some risks involved in maintaining the balance, by measuring model loads accurate determination of model attitude was possible as well as ensuring maximum design loads were not exceeded during testing.

A major objective of the AWS program² was to conduct free-to-roll testing on different fighter aircraft configurations that were known to either exhibit uncommanded lateral motions or not. The preproduction F/A18E and the AV-8B were chosen because these two aircraft exhibited wing-drop behavior. The two configurations that did not have wing drop were the F/A-18C and the F-16C. These models and their characteristics, shown in Fig. 2 and Table 1, had wing areas that ranged from 1.33 to 5.18 ft² and had weights that ranged from 55 to 490 lb. The sketches of the models shown in Fig. 2 are to the same scale in order to convey the relative model sizes used in the tests. To accommodate the estimated load requirements of the larger wind-tunnel models, the free-to-roll rig was designed for a maximum model normal force of 4000 lb. This load limit now allowed models to be tested at more typical Reynolds numbers of 2.5 to 4.5×10^6 per foot rather than the less than 10^6 per foot, which was required for tests in TDT with the previous free-to-roll apparatus.

To accomplish these requirements, it was decided to locate the new free-to-roll rig external to the model rather than internal as was done in previous applications. For internal model installations, several force balances with some form of rotational capability and varying load capabilities would have been required because all of the models had different size internal cavities where the force balances were located. The free-to-roll rig was designed to replace the standard sting butt⁹ in the Langley 16-ft. Transonic Tunnel such

Table 1 Characteristics of the four models

Parameter	AV-8B	F-18E/F	F-18C	F-16C
Length, in.	81.27	54.99	39.18	37.25
Wing area, ft ²	5.18	3.2	1.33	1.67
Span, ft	4.55	3.34	2.25	2.07
Weight, lb	490	185	55	56
Roll inertia, slugs-ft ²	4.0	1.2	0.2	0.2
Scale, %	15	8	6	6.67

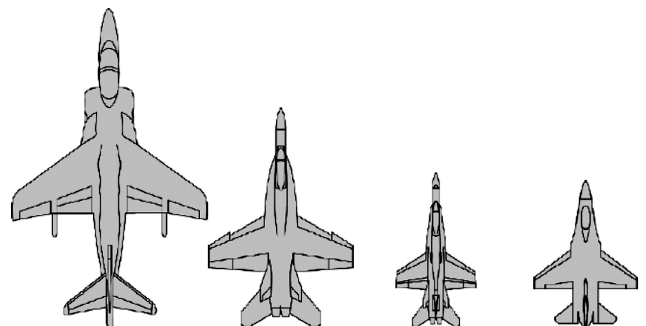


Fig. 2 Sketches of the four models.

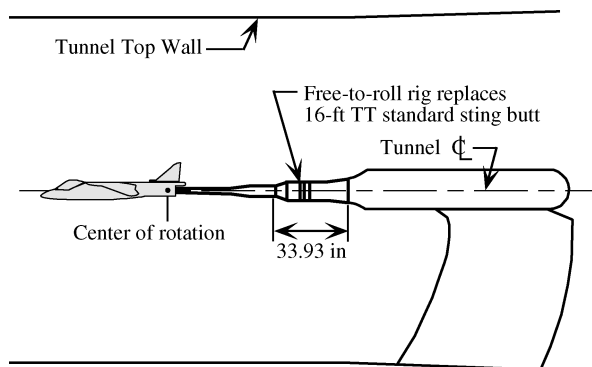


Fig. 3 Installation of free-to-roll rig in the Langley 16-Foot Transonic Tunnel.

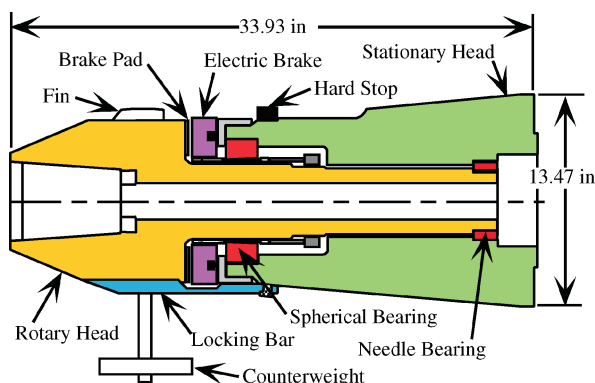


Fig. 4 Cross-sectional sketch of the free-to-roll rig.

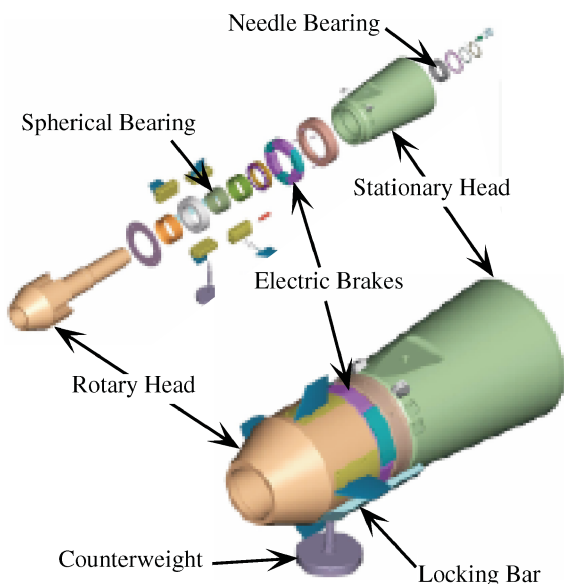


Fig. 5 Solid-body representation of the free-to-roll rig.

that a model and support sting could freely rotate about the longitudinal axis. A sketch showing the rig installed in the wind tunnel is shown in Fig. 3. Replacing the sting butt also meant that most existing and future models could be supported with the various sting/adapters arrangements typically used by the facility and that the model would always be located in the calibrated region of the test section.

Mechanical Design

A cross-sectional sketch of the rig is shown in Fig. 4, and a solid body and assembly representation of the mechanism are presented

in Fig. 5. The overall length was 33.93 in., and maximum diameter was 13.47 in. since the free-to-roll rig replaced the standard sting butt. The rig consisted of a rotary head that was supported in a stationary head with a forward spherical roller bearing and an aft needle bearing. This arrangement allowed for thermal expansion and some shaft flexibility without binding on the bearings and also allowed significant loading capability in excess of the 4000-lb load requirement already discussed. The spherical bearing had a load rating of 102,000 lb, and the needle bearing had a load rating of 15,600 lb. The rotary head was held onto the stationary head with a large carbon steel draw nut at the forward face of the stationary head. A single hard stop (with damping material) was located at the top center location as shown in Fig. 4. A locking bar was provided to rigidly fix the rotating head to the stationary head when static testing was required. Switching between the static to the FTR test mode took 30 min, which more than satisfied the requirement to change quickly test modes from conventional static testing to free-to-roll testing.

A roll resolver was used to measure roll angle. A 5:1 mechanical gear ratio amplified the roll-angle measurement. Roll angle can be resolved to 0.067 deg at FTR rig rates up to 1000 deg/s.

An adjustable counterweight assembly shown in Fig. 4 was provided to mass balance the model about the centerline of the support mechanism. The assembly consisted of a vertical rod to which varying weights could be secured. During preliminary testing in 16-ft TT of the free-to-roll rig without a model, large induced, nonrepeatable "aerodynamic tares" were found that could not be accounted for. Thus, the counterweight assembly was not used when tests were performed with a model attached to the free-to-roll rig.

The counterweight assembly was, however, used at wind-off conditions to determine system friction characteristics that result from friction in the bearings and any residual brake contact with the rotor. It is essential to know the magnitude of the friction moment because this moment can be a source of error when determining roll damping. Friction levels in the rig were determined by releasing the counterweight assembly with varying weights from an initial angular displacement and then analyzing the resulting roll-angle time histories. Additional estimates were made for each of the models prior to wind-on testing by measuring the rolling moments from the internally mounted balance and comparing those outputs with the calculated rolling moments based on roll acceleration of the model. These estimates showed some variation of friction between runs and some differences with loads on the rig. The friction was found to be small relative to the expected values of roll damping; however, the effects of friction will be greater for smaller models. The friction factors ranged from approximately 0.25 to 0.65 ft-lb/rad/s over the conditions evaluated.

Four actuated fins were provided to trim the model in roll. Each fin was mounted in a pivot block on the rotary head (Figs. 4 and 5) and was powered by a harmonic drive electric motor with a feedback encoder for fin position. The fins could be actuated independently or in unison. Preliminary testing of the rig without a model was conducted to determine roll control effectiveness of the fins and to ascertain if any uncommanded fin movement occurred or if fin "buzz" was present. It was known that these fins would introduce errors or tares into the FTR technique, but it was assumed that the tares would either be quantifiable or only have a slight adverse effect. Unfortunately, the fins produced unacceptable and nonrepeatable adverse effects and were removed and not used during subsequent tests of each of the four models. A fin with a different planform and or size could be developed that could provide desired trimming moments without introducing unacceptable tares.

Autobraking System

An independent braking system consisting of four 24-volt electric brakes was located in the space between the stationary and rotary heads as shown in Figs. 4 and 5. The brakes were mounted to the draw nut via pin posts much like brake calipers on automotive disc brakes. Brake pressure was applied to a wear plate mounted on the back of the rotary head by simply increasing current to the electromagnets inside the brakes. During extensive preliminary testing of

the free-to-roll rig in the model build-up bay at the 16-ft TT without a model mounted to the rig, it was found that the brakes did not completely disengage when the current to the brakes was turned off. As a result, sets of external springs were installed to pull the brakes back from the wear plate when they were not actuated.

Initially, control of the brakes was to be accomplished with the use of a simple on/off toggle switch. However, concerns were raised that very high torque loads would be imposed from applying the brakes during a sudden stop. While there was no indication that the brakes would grab when applied—that is, result in larger than expected braking torque for a given current level—this risk could be mitigated by “ramping up” the current provided to the brakes with the use of a computer-controlled, autobraking system.

For a symmetric model, the rolling moment was expected to be zero under operational conditions with no sideslip. However, experience had shown that large asymmetries in rolling moments occurred under abrupt-wing-stall conditions. For a very large model such as the AV-8B, these asymmetries could be as high as 150 ft-lb of torque and are indicative of the type of forcing functions present. However, under free-to-roll conditions the total rolling moment to be braked by the system model is determined by the combined inertia and aerodynamic rolling moments. For the design of the braking control system, the nominal dynamic stopping torque was assumed to be 140 ft-lb (at 5 rad/s velocity), and the maximum peak torque was 260 ft-lb.

Brake Control System

The brake control system was designed to both deploy the brakes at a specific roll angle and then hold the model at some position in presence of a rolling torque. A simple brake control law was designed where the brakes would deploy at a nominal braking current of 54% when some predetermined roll angle was reached and then the brake current would be ramped up to 100%. The brake control law was only dependent on measured roll angle ϕ and did not account for roll rate changes that can occur when the model is exposed to unanticipated roll accelerations from unsteady flow conditions at high angles of attack.

A schematic of the computer control braking system is shown in Fig. 6. This system continuously analyzed roll angle and roll rate from the resolver signal and then estimated the braking current required for given roll conditions. Model roll angle was determined with a roll resolver that had an accuracy of 7 min (gear ratio not accounted for). A “resolver card” in the brake computer not only provided excitation voltage, but also determined the final accuracy of roll angle, which was 4 arc minutes or 0.067 deg when the accuracies of the resolver card, resolver, and the 5:1 gear ratio are combined. The resolver card was custom made in order to accept the signals from the resolver shaft rotating at up to 5000 deg/s. The resolver itself had no speed limitation, but was limited by the resolver card in the brake computer. Roll angle can be resolved to 0.067 deg at FTR rig rates up to 1000 deg/s.

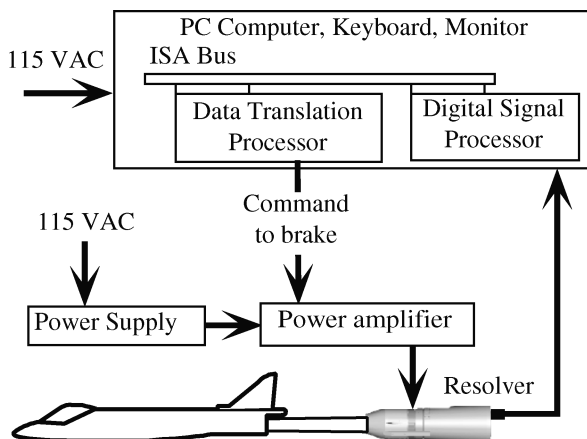


Fig. 6 Computer-controlled braking system.

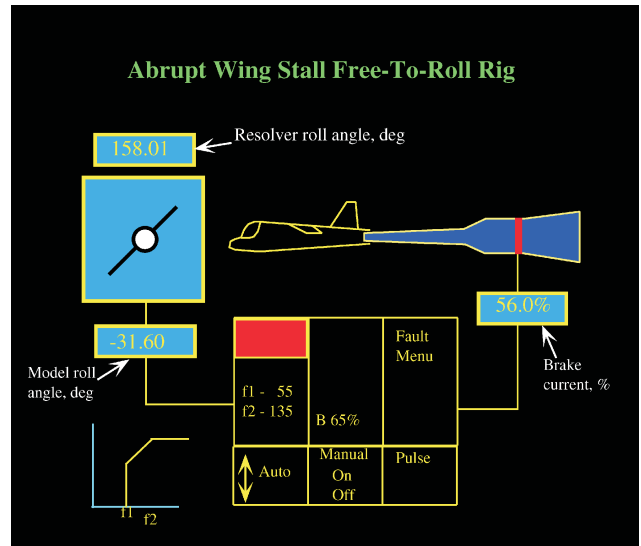


Fig. 7 Braking system display monitor.

Control Interface

The computer program also included a graphics mode screen shown in Fig. 7. The graphic displayed on the computer screen represented an animated picture of the status of the free-to-roll rig showing the roll attitude of the model in real time with an update rate of higher than 30 frames/s, which was acceptable from a persistence of vision point of view. The display also showed the status of various other elements of the system such as the raw resolver angle, brake current percent, and the status of mode control. Three modes of operation were possible and included:

- 1) In the auto mode, the model roll angle ϕ was compared with the set ϕ_1 , ϕ_2 , and based on the control logic a current was imposed on the brakes per the control law.
- 2) A brake-off mode or brake-on mode is available in the manual mode.
- 3) The pulse mode worked while on manual mode and in the auto mode only when the brakes are ON. The pulse mode, momentarily switches the brakes ON or OFF, to a state opposite of existing state. This mode was used to set a model to some predetermined bank angle.

Safety Analysis

Required Safety Analysis

All models tested in various wind tunnels at the Langley Research Center must adhere to the strict requirements set forth in Ref. 10. This guide contains criteria for the design, analysis, quality assurance, and documentation of wind-tunnel model systems including all model hardware, force balances, and external support systems. Because the free-to-roll rig involved a rotating system, further reviews of the mechanical design by a NASA Langley safety engineer were required. All model systems with rotating hardware were required to be designed for a system failure event, that is, the design shall be such that after an initial failure the model shall not experience any further failure that would cause facility damage during the tunnel shutdown process. Under this requirement, a failure of the independent braking system was not considered a safety issue because any rotation of the model would be halted with the mechanical hard stop. An issue was raised concerning the possibility of impact loading on the force balance if the model were to reach the stop, and an attempt was made to remove it. However, in the absence of any analysis, the safety engineer required the hard stop to be retained even though having the model essentially spinning was not considered a safety issue.

Additional stress analyses are required for the wind-tunnel model itself to account for inertial loads that would be imparted to key model components because of high accelerations in roll if the model is experiencing wing drop or rock.

Brake Analysis

A analysis of the braking system was performed to assure that the brakes could arrest the model assuming 1) a worst-case forcing function, 2) taking into account that the braking effectiveness was a function of time, and 3) integrating the resulting equation of motion about the body axis to predict a final bank angle ϕ at which the model would have come to rest. These analyses, which assumed ideal brake effectiveness, were not intended to be precise predictions of brake performance, but were only intended to be engineering estimates to show that the brakes could safely arrest the model before it would reach bank angles beyond 180 deg, which held true during the experiments.

The first task assumed a very conservative forcing function that would model the acceleration the model might experience in a wing-drop region. The forcing function, based on the data from the proof-of-concept experiment in the Langley TDT, was assumed to be between 4300 and 4900 deg/s² and occurred over a range of bank angles between $-45 \text{ deg} < \phi < 45 \text{ deg}$ depending on Mach number and model. This analysis was performed for two largest models tested, the AV-8B and the preproduction F/A-18E. Two separate modes were utilized to model brake effectiveness. The first mode assumed the computer controlled ramp function mode, whereas the second mode was based on the fact that the brakes took a finite time to energize as the coil was charged.

The analysis showed that for the AV-8B model with an assumed forcing function of 4300 deg/s² the model would achieve a roll rate of 120 deg/s and would come to rest at $\phi = 140$ to 160 deg depending on which braking mode was used. Similar results were found for the F/A-18E model. One result indicated by the brake analysis was that if a model were halted by the mechanical hard stop the impact load was such as to overload the roll component on the force balance. As a result, the hard stop was removed for all tests in order to remove the risk of damaging a balance. The only risk identified to a model spinning would be twisting of the various instrumentation leads with a possibility of the leads breaking which was not considered a safety issue.

Free-to-Roll Test Technique

The free-to-roll test technique is a single degree-of-freedom test method in which the model is free to roll about the longitudinal body axis. The overall objective of FTR testing is to identify early the potential of uncommanded lateral motion problems (or lack thereof). If the results of static force and moment tests through the use of static figures of merit¹¹ indicate that a potential exists for wing rock/drop, the FTR method can then be used to study the dynamic behavior. Inherently, the FTR technique evaluates unsteady, nonlinear aerodynamics and can be used to estimate the roll damping derivative. Figure 1 depicts the motions exhibited during the first phase of wing rock involving initial motions to the right. The airplane depicted in Fig. 1a is flying at zero sideslip and zero bank angle at some initial angle of attack. An acceleration in roll occurs (caused by an abrupt rolling-moment asymmetry or other disturbance), resulting in a rolling motion to the right. As the airplane rolls to the right about the body axis, the kinematics of the motion results in a reduction in airplane angle of attack and the generation of sideslip. When the airplane reaches a maximum right-wing-down attitude during the wing-rock cycle, the roll rate is zero, and the dihedral effect acts through the sideslip to create a restoring spring force to drive the airplane back to a wings-level condition. The restoring roll acceleration is a maximum at this point, and the airplane rolls back towards the wings-level condition. However, if the aerodynamic damping in roll (rolling moment caused by roll rate) is unstable, a residual roll acceleration to the left is present at the wings-level condition, and the cycle repeats to the left. Flow on the wing can be observed to reattach and separate during these motions, and the reattachment phenomena is especially visible during free-to-roll tests.

If the roll angle, roll rate, and roll accelerations that the wind-tunnel model experiences are to be scaled to flight, then certain specific dynamic similitude requirements must be met.¹² Obviously, for transonic testing Mach scaling must be used as in conventional

static tests. However, additional similitude requirements exist for FTR testing. "In Mach scaling, ability to satisfy attitude (e.g., α) scaling is dependent on satisfying Froude number similitude."¹² A static test requires model attitude, control deflection, Mach number, and Reynolds number similitude. In addition to these requirements, the FTR test also requires freestream velocity, dynamic pressure, inertia, reduced angular rate $pb/2V_\infty$, and Strouhal number similitude (if the motion of the model is oscillatory). The ability to Froude scale and Mach scale simultaneously is practically impossible in wind-tunnel testing (Ref. 12). The reduced angular velocity, Strouhal number, and freestream scaling requirements depend heavily on the geometric scale factor. Because the 16-ft TT is an atmospheric tunnel, the ratio of tunnel-to-flight freestream velocity is on the order of 1.1 for a flight altitude of 25,000 ft. As a result, the reduced angular velocity and Strouhal number are much lower than required to match flight conditions. The effect is that the change in local wing sectional angle of attack as a result of roll rate will not be as large as it should. Therefore, if the wing-rock motions occur in a highly nonlinear flow region the model will not experience as large a deviation in wing flowfield structure as the full-scale aircraft. This, in turn, could impact the amount of roll damping. A detailed discussion of the dynamic scaling issues for the specific models tested is addressed in Ref. 13.

There are two modes of testing utilized with the free-to-roll rig. First, conventional static testing is accomplished with the locking bar in place by measuring force and moment data using a six-component strain gauge balance over the desired angle-of-attack range. Model roll angle in this mode is determined from the standard instrumentation located within the model strut support system. The locking bar was then removed, and the FTR phase was conducted. During the FTR tests, in addition to the aforementioned measurements, roll-angle time histories were measured with a resolver having an accuracy of 0.067 deg, and videos of the rolling motions from three different views were also recorded.

During the FTR phase, three testing methods were utilized: continuous pitch sweeps, pitch pause, and ϕ offsets. The continuous pitch sweeps were conducted by slowly pitching the model up through the desired α range and then pitching the model back down through the α range while the model is free to roll. This method quickly identifies the α range where uncommanded lateral motion exists, if at all, and permits an assessment of any hysteresis effects in pitch angle. Various pitch rates were also used to assess pitch-rate effects on the development of the uncommanded lateral motions. As mentioned earlier, by maintaining the force balance and measuring model loads accurate determination of model attitude was possible as well as ensuring that maximum design loads were not exceeded during any phases of the free-to-roll testing.

Following the continuous pitch sweeps, pitch-pause points were taken to assess the lateral activity at specific pitch angles. In this procedure the model is held fixed with the wings level ($\pm 2 \text{ deg}$) using the brakes. The model is then moved to the desired pitch angle, whereupon the brakes are released and the ensuing model motion is recorded. The precursor continuous pitch sweeps are used to determine over what range of α that finer increments in θ are needed. The pitch-pause points are used to determine the tendencies of lateral motions to develop from a zero roll angle and zero-roll-rate condition. The ability to start from a predetermined pitch pause point with the brakes, provided a more rigorous assessment of potential lateral activity. This capability was not present in the previous FTR apparatus.

Next, the ϕ -offset points were obtained by releasing the model from rest at a non-zero sideslip condition, which induced a rolling motion by the action of the static lateral stability. This procedure is used to assess roll damping and can also ascertain if the model will develop sustained lateral activity even if no activity was originally detected when the model was released from a wings level position. After the brakes are released, the roll angle time histories of the resulting motions are analyzed to determine the roll damping characteristics of the model. Again, testing in this mode was made possible by the inclusion of a braking system in the new free-to-roll rig. Further details of these techniques as well as results of the tests

conducted on the four wind tunnel models can be found in Refs. 11 and 13.

One caution regarding the application of the FTR test technique is the use of the method at low pitch angles. During FTR testing, the wings are trimmed by the model's inherent static lateral stability ($C_{l_p} < 0$). If the model is disturbed from a wings-level condition at low pitch angles, the model could roll to large bank angles in order to generate enough rolling moment caused by sideslip to counter this disturbance. Therefore, at low pitch angles the rolling motions can be difficult to interpret, especially if the model has out-of-trim roll characteristics or if the wind tunnel has significant flow angularity.

Experimental Results

Correlation of Static to Free-to-Roll Forces

One of the FTR major requirements in the design of the free-to-roll rig was that the force balance be retained and used during testing. Even though there were risks involved with this requirement, having the force balance proved to be invaluable, in particular in determining accurately model attitude and from a safety standpoint in being able to monitor model loads during FTR testing. Another concern was that the forces and moments measured by the balance during free-to-roll testing could be erroneous. However, as will be shown, this turned out not to be the case. Comparisons of the measured forces and moments between static and FTR testing modes are presented in Figs. 8 and 9 for two conditions where the model did not or did have any lateral activity. The comparisons are for the AV-8B with the 65% LERX and 10-deg trailing-edge flap deflection at Mach numbers of 0.50 and 0.75. Although the results presented are for the largest model tested, they are typical for the other three configurations tested. The static tests were conducted in a pitch-pause mode, where data were recorded for 5 s at 10 frames/s. On the other hand, the FTR tests were conducted using the pitch-sweep mode, where data were recorded continuously at 100 frames/s. Excellent agreement is shown for the two test modes for the longitudinal data for both cases where uncommanded lateral activity was either not present or present. The longitudinal static data for these two cases are essentially equal to the time-averaged values from the free-to-roll test mode. However, large variations in the lateral coefficients exist when lateral activity was present such as that noted on Fig. 9 for the AV-8B at pitch angles between 10 and 15 deg. These large variations resulted from large changes in bank angle as the model experienced very severe wing rock. Although significant variations

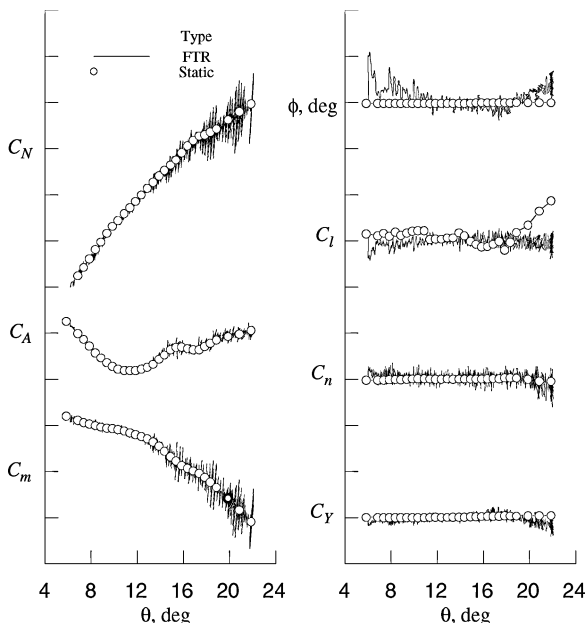


Fig. 8 Static/free-to-roll aerodynamics for AV-8B, 65% LERX, $\delta_{te} = 25$ deg, and $M = 0.50$.

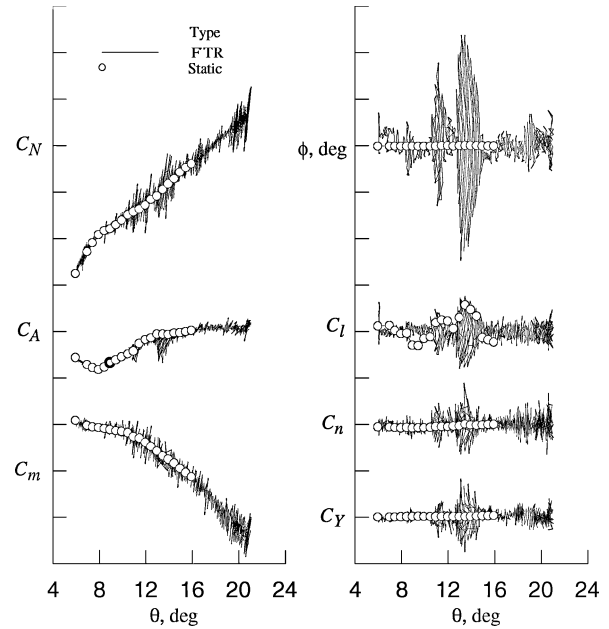


Fig. 9 Static/free-to-roll aerodynamics for AV-8B, 65% LERX, $\delta_{te} = 10$ deg, and $M = 0.75$.

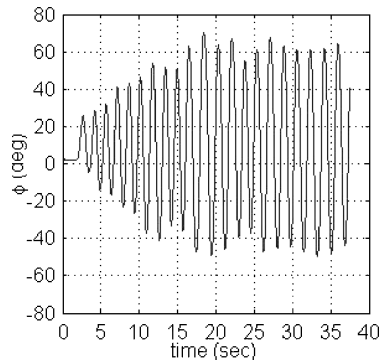


Fig. 10 Roll-angle time history showing wing rock for the AV-8B, 65% LERX, $\delta_{te} = 25$ deg, $M = 0.30$, and $\theta = 18.5$ deg.

in both normal force and pitching moment were present at $M = 0.50$ at θ greater than 15 deg (Fig. 8), these variations were caused by excessive model motion in pitch rather than in roll where amplitudes in bank angle were less than 5 deg.

Free-to-Roll Rolling Motions

Five types of rolling motion were observed during the free-to-roll testing of the four models shown in Fig. 2. These motions were categorized in Ref. 13, and interpretations were made as to possible causes based on a review of the static-force data, time-history traces of the roll angle, and estimations of roll damping C_{l_p} . All five types of motions can be initiated by abrupt (steady or unsteady) asymmetric wing stall. However, it was also seen that in some cases where abrupt asymmetric wing stall did not initiate the rolling motion from a wings level condition, the motion could be initiated by inducing a rolling motion through release of the model from a non-zero roll angle. Detailed discussions for each of these motions can be found in Ref. 13. Shown in this paper are two examples of these rolling motions: a sinusoidal motion defined as wing rock (Fig. 10), and an abrupt rolling motion damped with only one or two small amplitude overshoots that was designated wing drop (Fig. 11).

An example showing nearly limit-cycle wing rock is presented in Fig. 10 for the AV-8B with the 65% LERX, $\delta_{te} = 25$ deg, and $M = 0.30$. This motion (type 1 rolling motion¹³) is characterized as wing rock for which the amplitude range is fixed and does not vary with time. Such motions can occur when roll damping C_{l_p} is near zero. Only approximate limit-cycle type rolling motion was observed during tests.

Fig. 11 Roll-angle time history showing wing drop for the F/A-18E, flap set 6/8/4, $M = 0.80$, and $\theta = 7.3$ deg.

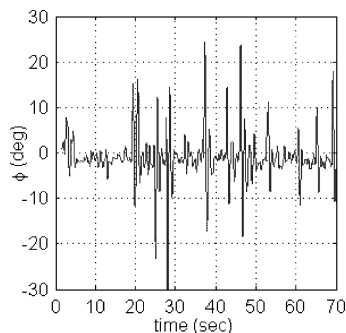


Figure 11 shows the roll-angle time history of the preproduction F/A-18E model at $M = 0.80$ with the 6/8/4 wing flap set where the first angle is the leading-edge flap deflection, the second angle is the trailing-edge flap deflection, and the third angle corresponds to the aileron bias. This is an example of rolling motions characterized by the occurrence of occasional wing drops (type 3 rolling motion¹³). Occasional means many seconds can occur between wing-drop events and where there was not any significant lateral activity. This type motion tends to occur on the edge of stall and well after the stall and is probably the result of unsteady variations in $C_{l,0}$ with highly stable $C_{l,p}$. At $M = 0.90$, the preproduction F/A-18E also experienced lateral events that consisted of frequent wing drops and damped wing-rock motions.¹³ This was in agreement with the wing-rock behavior found with the 9%, dynamically scaled model tested in the Langley Transonic Dynamics Tunnel at low Reynolds number.

Free-to-Roll Figure of Merit

A figure of merit was developed for free-to-roll testing in order to resolve levels of model lateral activity from inconsequential to significant. The first figure of merit used was a simple arbitrary color-coded rating system based only on amplitude of bank angle change.¹¹ However, taking into account amplitude alone could be misleading because the motion can have a large amplitude change but be so slow that it would be easily controlled. Taking into account just the magnitude of rates or accelerations alone could also lead to the wrong conclusions because a large acceleration with small amplitude oscillation might not be controllable but would not lead to a large deviation in the aircraft trajectory. Or, the acceleration might be favorable if it is returning the aircraft to a wings-level condition.

Therefore, a new figure of merit (FOM)¹³ was developed that accounted for both amplitude and rate. The FTR FOM is defined as the maximum absolute value of the amplitude change from a peak to its nearest valley divided by the time it takes to roll through this amplitude. This method captures wing drops that have no overshoots and wing rock that has sinusoidal motion. A color-coded system was also devised for this figure of merit, where for certain ranges of values for the FOM green represented inconsequential motions, yellow moderate motions, and red severe motions. Although still somewhat arbitrary, the various levels were established after a review of all of the results from the four models showed data falling predominantly within these three bands. This color-coded system was similar to that established during flight testing of the preproduction F/A-18E.¹⁴

Typical examples of the free-to-roll figures of merit are shown in Fig. 12 for the four configurations tested. Although the same range of the FTR FOM is used for all of the models, there is no expectation that the level of lateral activity means the same for all airplanes given their different sizes and inertias. As can be seen, moderate to severe lateral activity was found for both the AV-8B and preproduction F/A-18E. This was expected because these two airplane configurations were chosen for this investigation because they exhibited wing-drop behavior. Moderate to severe lateral activity also occurred for the F/A-18C between angles of attack from about 12.5 to 17 deg. However, at these angles of attack, the flaps are not on schedule and thus represent conditions that the airplane would not encounter

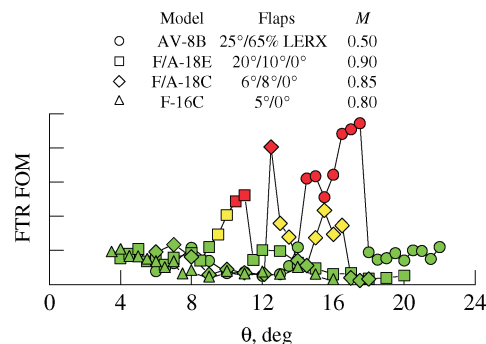


Fig. 12 FTR FOM ratings for selected configurations tested.

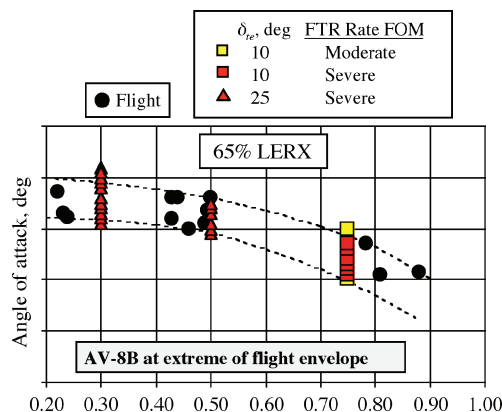


Fig. 13 Free-to-roll/flight comparison for AV-8B, 65% LERX.

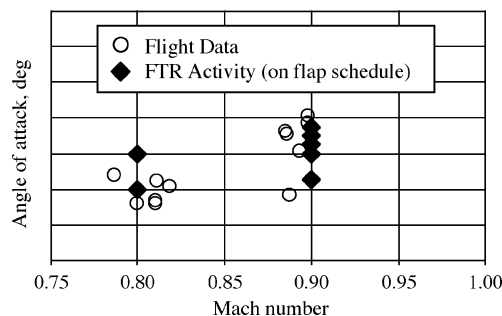


Fig. 14 Free-to-roll/flight comparison for preproduction F/A-18E.

in flight. For the flaps set shown, the flaps would be on schedule at $\alpha = 8.5$ deg, which is about 4 deg less than where lateral activity was noted. No lateral activity was observed for both the F/A-18C and F-16C for those test conditions when the flaps were on schedule, a result that is in agreement with flight.

Wind Tunnel to Flight Angle-of-Attack Correlation

Figure 13 shows a comparison between flight and wind tunnel for the AV-8B with the 65% LERX for those angles of attack where wing-rock/drop events occurred. The FTR lateral activity shown for the wind-tunnel data are for “yellow or red” conditions. There was no comparable system for the flight-test results. As can be seen, there is excellent agreement between the flight and wind-tunnel data. Similar results were found for the configuration with the 100% LERX at $M = 0.30$ and 0.75 (Ref. 11). Any wing-drop/rock activity noted was not considered an AV-8B aircraft operational problem.

A comparison of FTR activity between flight and wind tunnel for the preproduction F/A-18E is shown in Fig. 14 for Mach numbers of 0.8 and 0.9. The data shown are where both the airplane and model had approximately the same flap settings and Mach number at the time of a lateral activity event. As can be seen, there

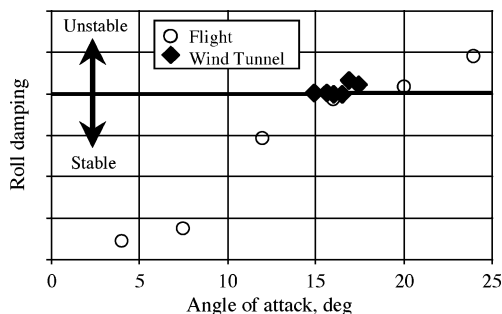


Fig. 15 Free-to-roll/flight comparison of AV-8B roll damping.

is good agreement between wind tunnel and flight. However, this correlation only shows unacceptable lateral activity, not the type of lateral activity. Note that although FTR lateral activity is present with flaps on schedule these results are for a model of the pre-production F/A-18E aircraft and are not representative of the production aircraft. The production airplane employs a modified wing leading-edge flap schedule and also has a porous fairing at the wing fold location that was not present on the preproduction F/A-18E model.

Although the AV-8B and the preproduction F/A-18E models were not dynamically scaled, the agreement of the FTR results with flight indicates that the models might not have to be dynamically scaled to make predictions of wing-drop/rock susceptibility.

Wind Tunnel to Flight Roll-Damping Correlation

A correlation of roll-damping between flight¹⁵ and that measured in the wind tunnel is presented in Fig. 15 for the AV-8B. Roll damping from the FTR tests was estimated from roll-angle time histories of the resulting motions when the model was released from some initial roll angle using parameter identification techniques.¹⁶ Good agreement is noted in Fig. 15. An analysis of the time histories at $M = 0.50$ (similar to Fig. 10 at $M = 0.30$) indicated that the severe wing rock the AV-8B experienced resulted from a loss of roll damping.¹³

Summary

A new free-to-roll test rig has been designed and built for transonic testing as part of the NASA/Navy Abrupt Wing Stall Program. The major design requirement for the new free-to-roll test rig was to be able to use existing industry high-strength wind-tunnel models of varying sizes, weights, and maximum load capabilities. In addition, conventional static tests and free-to-roll tests were to be conducted in a relatively rapid sequence during a specific tunnel entry utilizing the same model and tunnel test apparatus. The overall objective was to demonstrate the utility of the free-to-roll test technique as a tool for identifying areas of significant uncommanded lateral activity during ground testing and for gaining insight into the wing-drop and wing-rock behavior of military aircraft at transonic conditions. The following summarizes the major findings of this study:

- 1) The free-to-roll rig met or exceeded all design requirements with no operational limitations.
- 2) The free-to-roll test rig was used successfully to assess the static and dynamic characteristics of four different configurations—two configurations that exhibited uncommanded lateral motions (pre-production F/A-18E and AV-8B) and two that did not (F/A-18C and F-16C).

3) The lateral activity observed during testing was categorized as being either wing-drop or wing-rock motions.

4) A figure of merit was developed to discern the severity of lateral motions. Using this figure of merit, it was shown that the free-to-roll test technique identified conditions where lateral activity occurred for the AV-8B and preproduction F/A-18E that correlated with flight. The figure of merit predicted no significant lateral activity for the F/A-18C and F-16C on flap schedule, which is in agreement with flight.

5) The loss of roll damping experienced by the AV-8B full-scale aircraft at high angles of attack was predicted using the free-to-roll test technique.

Acknowledgments

The authors would like to thank Joseph Chambers for motivating the use of the free-to-roll technique in the transonic speed regime. The computer-controlled automatic braking system was designed by Sundaeswara Balakrishna of Vigyan, Inc.

References

- ¹Chambers, J. R., and Hall, R. M., "Historical Review of Uncommanded Lateral-Directional Motions at Transonic Speeds," *Journal of Aircraft*, Vol. 41, No. 3, 2004, pp. 436–447; also AIAA Paper 2003-0590, Jan. 2003.
- ²Hall, R. M., and Woodson, S., "Introduction to the Abrupt Wing Stall (AWS) Program," *Journal of Aircraft*, Vol. 41, No. 3, 2004, pp. 425–435; also AIAA Paper 2003-0589, Jan. 2003.
- ³Hall, R., Woodson, S., and Chambers, J., "Accomplishments of the AWS Program and Future Requirements," AIAA Paper 2003-0927, Jan. 2003.
- ⁴Chambers, Joseph R., and Anglin, Ernie L., "Analysis of Lateral-Directional Stability Characteristics of a Twin-Jet Fighter Airplane at High Angles of Attack," NASA TN D-5361, May 1969.
- ⁵Murri, D. G., Nguyen, L. T., and Grafton, S. B., "Wind-Tunnel Free-Flight Investigation of a Model of a Forward-Swept Wing Fighter Configuration," NASA TP-2230, Feb. 1984.
- ⁶Nguyen, L. T., Yip, L., and Chambers, J. R., "Self-Induced Wing Rock of Slender Delta Wings," AIAA Paper 81-1883, Aug. 1981.
- ⁷Brandon, J. M., Murri, D. G., and Nguyen, L. T., "Experimental Study of Effects of Forebody Geometry on High Angle of Attack Static and Dynamic Stability and Control," *International Council of the Aeronautical Sciences 15th Congress Proceedings*, Vol. 1, 1986, pp. 560–572.
- ⁸Hwang, C., and Pi, W. S., "Some Observations on the Mechanism of Aircraft Wing Rock," AIAA Paper 78-1456, Aug. 1978.
- ⁹Capone, Francis J., Bangert, Linda S., Asbury, Scott C., Mills, Charles T., and Bare, E. Ann, "The NASA Langley 16-Foot Transonic Tunnel—Historical Overview, Facility Description, Calibration, Flow Characteristics, Test Capabilities," NASA TP-3521, Sept. 1995.
- ¹⁰"Wind-Tunnel Model Systems Criteria," NASA LAPG 1710.15, 27 Sept. 2000.
- ¹¹Capone, F. J., Hall, R. M., Owens, B., Lamar, J. E., and McMillin, S. N., "Review and Recommended Experimental Procedures for Evaluation of Abrupt-Wing-Stall Characteristics," *Journal of Aircraft*, Vol. 41, No. 3, 2004, pp. 448–455; also AIAA Paper 2003-0922, Jan. 2003.
- ¹²Wolowicz, C. H., Bowman, J. S., and Gilbert, W. P., "Similitude Requirements and Scaling Relationships as Applied to Model Testing," NASA TP 1435, July 1979.
- ¹³Owens, B., Capone, F. J., Hall, R. M., Brandon, J., and Cunningham, K., "Free-to-Roll Analysis of Abrupt Wing Stall on Military Aircraft at Transonic Speeds," AIAA Paper 2003-0750, Jan. 2003.
- ¹⁴Roesch, M., and Randall, B., "Flight Test Assessment of Lateral Activity," AIAA Paper 2003-0748, Jan. 2003.
- ¹⁵Stevenson, S. W., Holl, D., and Roman, A., "Parameter identification of AV-8B Wingborne Aerodynamics for Flight Simulator Model Updates," AIAA Paper 92-4506-CP, Aug. 1992.
- ¹⁶Morelli, E. A., "System Identification Programs for Aircraft (SIDPAC)," AIAA Paper 2002-4704, Aug. 2002.